Ionic Currents in Two Strains of Rat Anterior Pituitary Tumor Cells

JANET M. DUBINSKY and GERRY S. OXFORD

From the Department of Physiology and The Neurobiology Program, University of North Carolina at Chapel Hill, Chapel Hill, North Carolina 27514

ABSTRACT The ionic conductance mechanisms underlying action potential behavior in GH3 and GH4/C1 rat pituitary tumor cell lines were identified and characterized using a patch electrode voltage-clamp technique. Voltage-dependent sodium, calcium, and potassium currents and calcium-activated potassium currents were present in the GH3 cells. GH4/C1 cells possess much less sodium current, less voltage-dependent potassium current, and comparable amounts of calcium current. Voltage-dependent inward sodium current activated and inactivated rapidly and was blocked by tetrodotoxin. A slower-activating voltage-dependent inward calcium current was blocked by cobalt, manganese, nickel, zinc, or cadium. Barium was substituted for calcium as the inward current carrier. Calcium tail currents decay with two exponential components. The rate constant for the slower component is voltage dependent, while the faster rate constant is independent of voltage. An analysis of tail current envelopes under conditions of controlled ionic gradients suggests that much of the apparent decline of calcium currents arises from an opposing outward current of low cationic selectivity. Voltage-dependent outward potassium current activated rapidly and inactivated slowly. A second outward current, the calcium-activated potassium current, activated slowly and did not appear to reach steady state with 185-ms voltage pulses. This slowly activating outward current is sensitive to external cobalt and cadmium and to the internal concentration of calcium. Tetraethylammonium and 4-aminopyridine block the majority of these outward currents. Our studies reveal a variety of macroscopic ionic currents that could play a role in the initiation and short-term maintenance of hormone secretion, but suggest that sodium channels probably do not make a major contribution.

INTRODUCTION

Mammalian pituitary cells have been found to exhibit an electrical excitability similar to that of neural and muscle cells. Both spontaneous and evoked electrical activities have been recorded in various clonal pituitary cells maintained in tissue culture. Sodium- and calcium-dependent action potentials have been reported in the GH3 cell line by Biales et al. (1977) and Ozawa and Miyazaki (1979) and in

Address reprint requests to Dr. Gerry S. Oxford, Dept. of Physiology, School of Medicine, Medical Research Wing 206 H, The University of North Carolina, Chapel Hill, NC 27514.

J. GEN. PHYSIOL. © The Rockefeller University Press · 0022-1295/84/03/0309/31 $1.00

Volume 83 March 1984 309–339

AtT/20 cells by Adler et al. (1983). Other investigators have reported only calcium-dependent activity with no indication of a tetrodotoxin (TTX)-sensitive Na component (Kidokoro, 1975; Dufy et al., 1979*a*; Taraskevich and Douglas, 1980). The ionic basis of action potentials in these cells is of functional importance when considering possible mechanisms by which various agents such as thyrotropin-releasing hormone (TRH), dopamine, or estrogen act on these cells to stimulate hormone release and to alter the firing frequency (Kidokoro, 1975; Dufy et al., 1979*a*, *b*; Ozawa and Kimura, 1979; Taraskevich and Douglas, 1980; Kaczorowski et al., 1983).

In order to better understand the events occurring at the membrane level in response to these agents, direct recording of the separate membrane currents present in cultured pituitary cells is necessary. While previous voltage-clamp studies of particular current components from GH3 cells have been reported (Dufy and Barker, 1982; Hagiwara and Ohmori, 1982), no comprehensive description of the various ionic currents has been attempted. We view this as a necessary first step towards discriminating possible target sites of action of the modulatory hormones. Therefore, the aim of this work is to identify the ionic conductance mechanisms present in the GH3 cell line and its subclone, GH4/C1.

The "gigohm seal" patch-clamp technique (Hamill et al., 1981) has been employed to record whole cell currents under voltage-clamp conditions from GH3 and GH4/C1 cells maintained in culture. We report here that these cell lines possess voltage-dependent potassium and calcium channels and calcium-dependent potassium channels. In addition, the GH3 cell line possesses voltage-dependent sodium channels. A preliminary report of this work has appeared elsewhere (Dubinsky and Oxford, 1982).

METHODS

The GH3 rat pituitary tumor cell line was obtained from the American Type Culture Collection, Rockville, MD, and a subclone, GH4/C1, was kindly provided by Dr. Priscilla Dannies, Yale University. Both cell lines were maintained at 37°C in a humidified atmosphere of 5% CO_2, 95% air. Every 3–4 d, cells were fed Ham's F10 nutrient medium supplemented with 15% horse serum, 2 mM glutamine, 6 mg/ml glucose, and 20–50 μg/ml gentamycin. GH3 cell medium also contained 2.5% fetal calf serum. It has been found that GH4 cells increase their secretory activity without fetal calf serum (P. S. Dannies, personal communication). Control electrophysiological experiments were performed in which media formulations for the two cell lines were switched and no differences were observed with respect to the results presented below. Seeding cells were removed from stock flasks by gentle aspiration and plated on plastic coverslips in 35-mm polystyrene petri dishes and used for electrophysiology 2–10 d after plating.

Recording solutions varied greatly, depending on the ion substitution experiment being performed. The basic extracellular salt solution employed contained 150 mM NaCl, 5 mM KCl, 2 mM $CaCl_2$, 1.3 mM $MgCl_2$, 10 mM glucose, and 5 mM Hepes. The basic intracellular solution contained in the recording electrode was composed of 130 mM K-aspartate, 20 mM KCl, 10 mM glucose, and 5 mM Hepes. Variations from these standard solutions are noted in the figure legends. All solutions were adjusted to pH 7.2–7.4. Calcium buffering was accomplished with EGTA. The Ca-EGTA equilibria were calculated using the dissociation constants given by Sillen and Martel (1964), taking into

consideration the Mg^{2+} and H^+ ion concentrations. The osmolarity of these solutions was carefully monitored such that intracellular osmolarity ranged from 292 to 298 mosmol and extracellular osmolarity was in the range of 295–305 mosmol. Optimal recordings were made from cells in which the pipette intracellular solution was 5–10 mosmol hypoosmotic with respect to the extracellular solution. External solution flowed into the experimental chamber through a gravity-flow system at a rate of 1 ml/min. The chamber solution volume was 0.5–1.0 ml, depending on the solution height. Solution changes in the chamber were completed within 3 min; cells close to the solution inflow were routinely chosen for recording to ensure that solution changes at the cell being studied were as rapid as possible. All experiments were performed at room temperature. The experimental chamber was mounted on the fixed stage of an inverted microscope equipped with Nikon optics modified for Hoffman modulation contrast. Cells were viewed at a magnification of 400.

Ionic current recordings were obtained using the patch electrode voltage-clamp method of Hamill et al. (1981), employing a similar circuit and a 1-GΩ feedback resistor. The current response to a voltage step settled in 300 μs. The whole cell current recording configuration was used on single isolated GH3 or GH4 cells. 3–10-MΩ patch electrodes were pulled from Boralex glass microcapillary pipettes (Rochester Scientific Co., Rochester, NY) and coated with Qdope (GC Electronics, Rockford, IL) to within 30–50 μm of the tip to reduce stray electrode capacitance. After initial formation of a gigohm seal between the patch pipette and the cell surface, capacitance compensation was added to null out the current surge caused by the remaining capacitative coupling of the patch electrode to the bath. At this point, spontaneous extracellular "action currents" could often be recorded through the membrane patch as well as a variety of single-channel currents. An additional pulse of suction was then applied to rupture the membrane beneath the pipette tip, permitting the electrode access to the intracellular milieu. Diffusion of ions between the pipette and the cell interior occurred so rapidly that internal dialysis was complete by the time all the preliminary measurements of passive electrical properties and morphology were noted (20–60 s). This was especially obvious when cesium or other cationic blockers of outward current were in the pipette and no outward currents were seen in response to the first depolarizing voltage pulse.

Sometimes the pipette opening was partially occluded by membrane fragments, resulting in a large resistance in series with that of the cell membrane. If the error introduced by this resistance could not be effectively reduced by additional suction or positive feedback compensation, the cell was discarded. Typical series resistance values after compensation were 3–10 MΩ compared with a cell input resistance of 1–12 GΩ. For 100-pA inward currents, this would yield a maximum error of 1.0 mV. For outward currents, which could reach 600–800 pA at the extremely high voltages, a 6–8-mV error may be present. In such cases the currents reported for high voltages are underestimates of the true values. In all cells where tail current measurements were critical, the series resistance values were <6 MΩ. During the course of an experiment, cell cytoplasm often migrated into the patch pipette, further increasing series resistance errors. If this could not be similarly compensated, the cell was discarded. Careful adjustment of pipette openings and solution osmolarities usually prevented such cytoplasmic migration.

The cell's current responses to voltage pulses were low-pass-filtered at 10 kHz, digitized, and stored using a PDP 11/03 computer (Digital Equipment Corp., Marlboro, MA). The computer also controlled delivery of the voltage pulses via a programmable stimulator. Currents were sampled at 20-, 50-, or 100-μs intervals.

For these small high-resistance cells, the response to a voltage step contained a large capacitative current component as well as ionic currents. The typical settling time for this

capacitative current was 2–3 ms. To remove this capacitative artifact and any linear leakage current, pulse protocols contained an initial depolarizing voltage step followed by four hyperpolarizing pulses of one-quarter the test pulse amplitude. The current responses to all five of these pulses were summed by the computer before final storage. Currents during the hyperpolarizing pulses displayed no time-dependent activity (Fig. 2*B*). In some cases, when the analog-to-digital converters were saturated by the capacitative current, this subtraction procedure was imperfect. For the majority of cells, however, ionic membrane currents could be resolved up to 400 μs following a voltage step.

Gigohm seal formation and intracellular access were obtained with the membrane voltage-clamped to the system's junction potential. This junction potential was defined as the potential of the electrode with respect to the bath for which no current flowed before the electrode approached a cell. Once intracellular access was obtained, ionic membrane currents were activated. A hyperpolarizing DC potential was applied until no net membrane currents were observed. This potential relative to the bath potential was taken to represent the resting membrane potential of the cell. The cell was further hyperpolarized to a −60-mV holding potential from which various voltage pulse protocols were applied. Holding currents were typically 5–6 pA. Junction potential changes introduced by solution changes were measured after completion of the experiment and voltages were corrected accordingly. Such junction potential changes were usually of the order of 0–3 mV.

TABLE I

Passive Membrane Properties

	V_m	R_m	C_m	Diameter
	mV	*GΩ*	*pF*	*μm*
GH3	−42.6±12.2 (127)*	4.2±2.9 (176)	9.78±2.59 (176)	13.8±1.5 (106)
GH4	−49.6±14.0 (74)‡	4.2±3.2 (85)	7.82±2.53 (85)‡	13.9±1.7 (74)

* Values are expressed as means ± standard deviation with the number of cells in parentheses.
‡ GH4 values that are significantly different from GH3 values ($P < 0.001$).

Passive cell membrane properties were calculated from the current response to small hyperpolarizing pulses. After electronic compensation for the electrode capacitance, the integral of the current transient in response to small hyperpolarizing pulses was divided by the voltage step to yield the cell membrane capacitance. The sum of the membrane resistance, in parallel with the seal resistance, and the electrode series resistance can be calculated from the steady state current. To estimate the contribution of the series resistance alone, single exponentials were fit to the transient current response and extrapolated back to the onset of the hyperpolarizing voltage step. Where statistical comparisons were made, a two-tailed Student's *t* test was applied to the means of the measurements.

RESULTS

Passive Membrane Properties

Passive membrane properties measured using small hyperpolarizing voltage pulses are presented in Table I. The values for membrane resistance are considerably higher than those previously reported for these cells in studies using microelectrode impalements (e.g., 500 MΩ in Taraskevich and Douglas, 1980). This difference may be attributable to current leakage around the site of

microelectrode impalement in previous studies. The membrane capacitance values correspond to specific membrane capacitances of 1.27 ± 0.41 $\mu F/cm^2$ (mean ± SD) for GH4 cells and 1.59 ± 0.42 $\mu F/cm^2$ for GH3 cells, assuming an average cell diameter of 14 μm. It is noteworthy that for cells of similar size, there is not a significant difference between GH3 and GH4 membrane resistances, although the membrane capacitances are significantly different. Published transmission electron microscopic studies of GH3 cells do not reveal any infoldings of the plasma membranes (Tixier-Vidal et al., 1975). The variability in membrane capacitances of both cell lines may correspond to the often irregular appearance of the cell surfaces as seen under Hoffman modulation contrast optics.

The resting membrane potential values reported here are the zero-current potentials as described in the Methods. They may not reflect the actual resting membrane potential, since this is reported to fluctuate with the spontaneous activity recorded in these cells (Kidokoro, 1975). However, the value of zero-current potential for GH3 cells does agree remarkably well with the membrane potentials reported in the microelectrode studies (e.g., −40 ± 2 mV in Taraskevich and Douglas, 1980). The zero-current potentials for GH4 cells are significantly greater than for GH3 cells.

Inward Ionic Currents

In a voltage-clamped GH cell, depolarizing voltage steps elicit time- and voltage-dependent membrane ionic currents in both inward and outward directions. The traces in Fig. 1*A* illustrate membrane currents uncorrected for capacitative and leakage current. Hyperpolarizing voltage steps elicited only capacitative current and a small steady state linear leakage current (Fig. 1*B*).

Inward currents were examined in the absence of large outward currents when cesium was employed as the intracellular cation inside the pipette. Although intracellular *N*-methylglucamine (NMG), tetramethylammonium, sodium, and lithum all effectively blocked the outward currents, cesium was the most convenient intracellular cation to use for these experiments as it yielded lower, less variable junction potentials and longer cell viability. Under these conditions, inward currents in GH3 cells were composed of fast- and slow-activating components (Fig. 2). The fast component inactivated rapidly and disappeared altogether when 10^{-6} M TTX was added to the external bath (Fig. 2*A*). Typically, 10^{-7} M TTX blocked this fast inward current. In other cells the slow component was abolished by the addition of 2 mM cobalt (Fig. 2*B*). On the basis of this initial pharmacological separation, the fast and slow components were tentatively identified as voltage-dependent sodium and calcium channels, respectively.

SODIUM CURRENTS Sodium currents were studied in the absence of inward calcium current in calcium-free solutions containing either Mg^{2+} or Co^{2+}. Fig. 3 illustrates sodium currents which are inward for low depolarizations and which become outward with larger depolarizing steps. The characteristic activation-inactivation sequence seen in sodium currents in other preparations is present in GH3 cells. When the external concentration of sodium is decreased, the peak amplitude of the fast inward current is reduced. Current-voltage plots for peak

inward sodium current exhibit a clear shift in reversal potential for changes in the external sodium concentration (Fig. 4*A*). These shifts in reversal potential agree reasonably well with those expected from a purely Nernstian relationship (Fig. 4*B*). This indicates that sodium is the principal current carrier for the fast component of inward current.

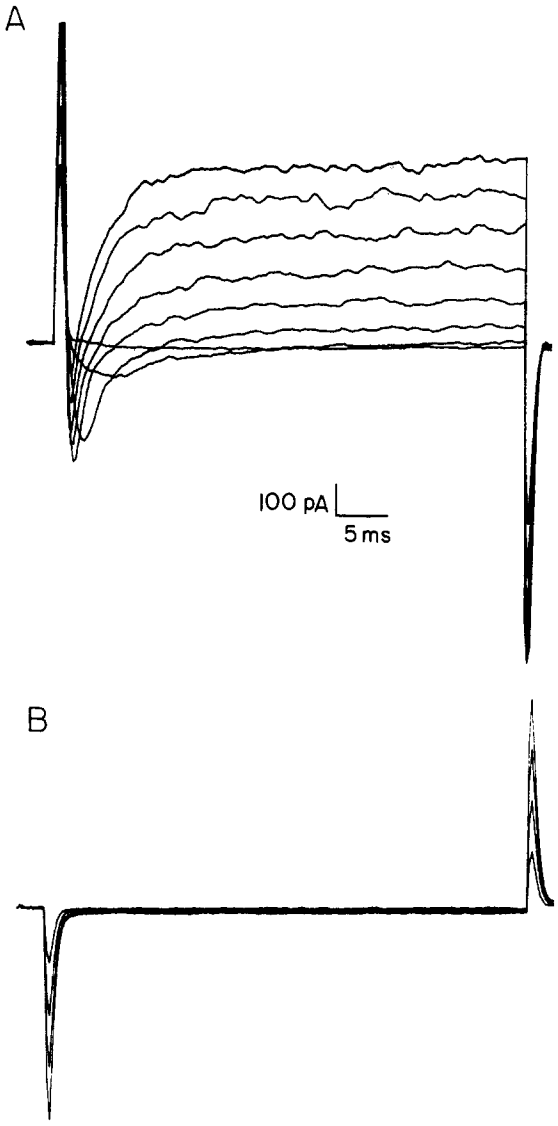

FIGURE 1. Whole cell currents in normal internal and external solutions for 45-ms voltage steps to −28.5, −18.5, −8.5, 1.5, 11.5, 21.5, 31.5, and 41.5 mV from a holding potential (V_H) of −58.5 mV. Records are uncorrected for capacitative and leakage currents. Note the increase in "noise" in outward currents of increasing magnitude over that seen in the baseline current. GH3 cell 1/8/82-1.

Because the onset of I_{Na} at high voltages was sometimes occluded by the residual capacitative transient, a detailed study of the activation kinetics was not undertaken. However, the voltage dependence of inactivation was examined. A test pulse to 24 mV was preceded by a 700-ms conditioning pulse of variable amplitude. Between these two pulses the membrane potential was returned to the holding potential of −60 mV for 1 ms. The peak Na current response to the test pulse was normalized with respect to the maximum peak I_{Na} and plotted against the prepulse voltage in Fig. 5. For four GH3 cells, the average value of

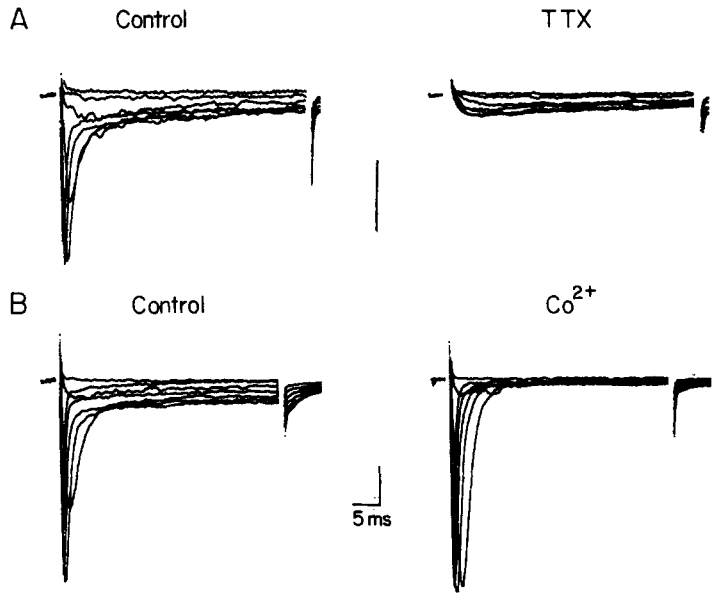

FIGURE 2. Inward currents show two components in GH3 cells. (*A*) Inward currents in normal external solution before (left) and after (right) 10^{-6} M TTX was added externally. Voltage steps were to −34, −25, −14, −4, 6, 16, and 26 mV from a V_H of −74 mV. Internal solution (mM): 150 Cs^+, 150 $aspartate^-$, 5 Hepes, and 5 glucose. Cell 2/5/82-1. (*B*) Inward currents in normal external solution before (left) and after (right) addition of 2 mM $CoCl_2$, externally for voltage steps to −42, −32, −22, −12, −2, 8, and 18 mV from a V_H of −62 mV. Internal solution (mM): 150 NMG^+, 150 $aspartate^-$, 5 Hepes, and 5 glucose. Cell 2/9/82-4. Records from both cells are uncorrected for leakage currents. The vertical scale bar in both cases represents 100 pA.

the voltage for half-maximal steady state inactivation ($V_{0.5}$) was −51 ± 6 mV. This inactivation curve indicates that at an average resting potential of −43 mV, only 35% of the sodium channels in GH3 cells are available to activate and contribute to action potential generation. This suggests that the sodium current may not be essential for spontaneous activity observed in GH3 cells. Correspondingly, spontaneous activity in the form of action currents, recorded extracellularly after gigaseal formation and before rupture of the cell membrane, have been recorded in our system in both the presence and absence of TTX. The relative

inability of the sodium channel to contribute to action potential generation caused by resting inactivation may explain the previous conflicting reports of both Na-dependent and Na-independent action potentials in GH3 cells (Kidokoro, 1975; Biales et al., 1977; Ozawa and Miyazaki, 1979; Dufy et al., 1979*a*; Taraskevich and Douglas, 1980).

Peak inward sodium current in GH3 cells measured at +12 mV from a holding potential of −60 mV ranged from −89 pA in a 14-μm-diam cell to −471 pA in a 12-μm cell. If the average single sodium channel current is assumed to be 0.77 pA (extrapolated to +12 mV from values given in Horn et al., 1982), then these currents reflect the opening of 116–612 channels per cell. If it is further assumed that of the 94% of the channels available to open at the holding potential of −60 mV, 50% are activated by a voltage step to 12 mV (P_0 = 0.5; Fenwick et al., 1982), then the total number of Na channels ranges from 246 to 1,301 channels

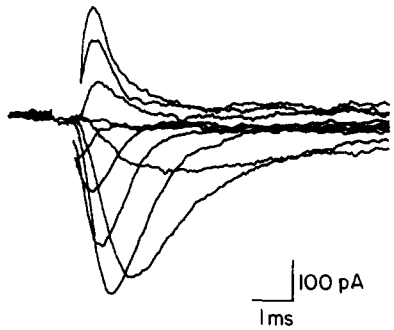

FIGURE 3. Reversal of sodium currents recorded from a GH3 cell for 12-mV voltage steps from −24 to + 84 mV from a V_H of −60 mV. Each trace represents a single sweep taken at each voltage. Imperfect subtraction of the capacitative transient caused spurious points which were not printed in several traces. External solution contained (mM): 150 NaCl, 5 KCl, 2 $CoCl_2$, 10 glucose, and 10 Hepes. Internal solution contains (mM): 50 Na^+, 100 Cs^+, 130 aspartate$^-$, 20 Cl^-, 10 glucose, and 10 Hepes. Cell 3/11/83-8.

per cell. If these channels are evenly distributed over a perfectly spherical cell, this represents a density of 0.40–2.88 channels/μm^2.

CALCIUM CHANNEL CURRENTS The slow component of inward current was studied in the presence of 3×10^{-7} M TTX. Both calcium and barium are current carriers for this slow inward current. The amplitude of barium current exceeded that of calcium current for equal concentrations of these divalent cations, as illustrated in Fig. 6. Increasing the external concentrations of calcium or barium also increased the inward current amplitude for the same cell (not illustrated here). It was difficult to perform more than one solution change when studying these calcium currents since they irreversibly diminished in amplitude over 10–20 min and eventually disappeared altogether. This "rundown" is seen in the recovery current-voltage curve for barium current in Fig. 6*E*. Addition of EGTA, cGMP, cAMP, Mg-ATP, and/or glutathione to the pipette intracellular solution did not qualitatively prolong the life of these currents. For this

reason, multiple current amplitude comparisons for different divalent cation concentrations were not attempted. In addition to the block of this slow inward current by cobalt as illustrated in Fig. 2*B*, cadmium, manganese, zinc, or nickel (1 mM) were also effective as blocking agents. The block by Co^{2+}, Mn^{2+}, and

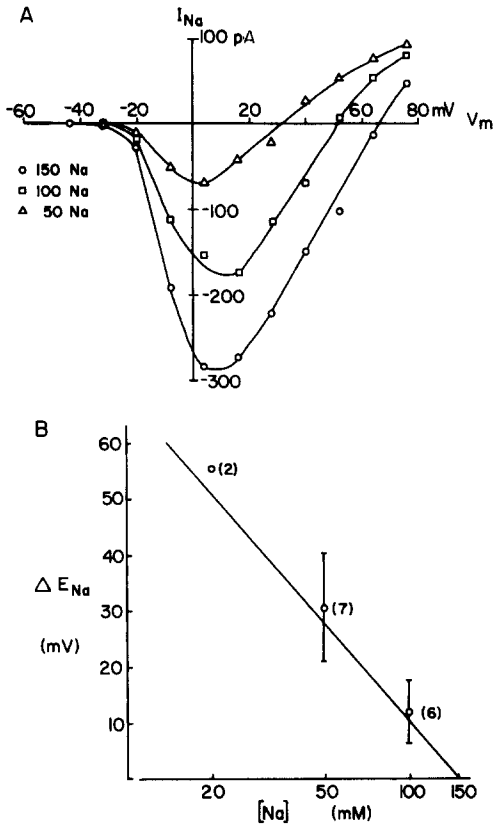

FIGURE 4. Shift of the sodium current reversal potential with changes in external Na concentration. (*A*) Peak sodium current-voltage relationships in various external [Na]. External solutions contained (mM): 10 $MgCl_2$, 10 glucose, 5 Hepes, and either 50, 100, or 150 Na^+. External sodium concentration was adjusted on an equimolar basis by substitution of NMG. Internal solution (mM): 110 Cs^+, 50 Na^+, 160 $aspartate^-$, 7 glucose, and 5 Hepes. Cell 3/29/82-1. (*B*) Shift in E_{Na} plotted as a function of log [Na]. E_{Na} values were corrected for junction potentials. Number of cells at each concentration are shown in parentheses. The line through data points represents the theoretical Nernst relationship at 23°C.

Ni^{2+} was reversible. Reversal of the block by Cd^{2+} or Zn^{2+} was not attempted. It is concluded that the slow component of inward current is a voltage-dependent calcium current similar in nature to calcium currents in other excitable membranes (Hagiwara and Byerly, 1981).

The peak *I-V* curves for divalent ion currents could not be fit by chord

conductances even in those cells where clear reversal potentials were observed. Permeabilities, calculated according to the constant field equation (Goldman, 1943; Hodgkin and Katz, 1949) from peak current values, fit well and saturated at potentials above +60 mV (Fig. 7*A*). When the P_{Ca}-V curve is linearized according to the transform log $[P/(P_{max} - P)]$ and plotted vs. voltage, the slope indicates an e-fold increase in permeability for a 10.7 ± 0.7 mV (n = 6) increase in voltage.

Instantaneous current-voltage measurements were obtained in response to a voltage change from a fixed prepulse level (+24 mV) to a variable test pulse amplitude. Calcium tail currents, measured after the end of the prepulse in response to the test pulse, clearly contained two exponential components (Fig. 8*A*). The instantaneous I_{Ca} was calculated by extrapolating an exponential fit to the early component of the measured current response back to the onset of the

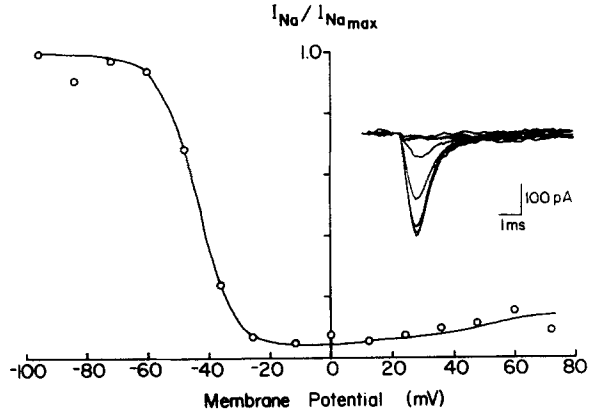

FIGURE 5. Voltage dependence of sodium current inactivation in GH3 cells. Inset: inward current records for test voltage steps to +24 mV preceded by 700-ms conditioning pulses to the voltages indicated on the abscissa. A "gap" of 1 ms at the holding potential (−60 mV) separates conditioning and test pulses. The data points are peak sodium current values from these records normalized to the maximum value. The smooth curve through data points was fit by eye. Same cell as in Fig. 3.

voltage step. The instantaneous I-V curve presented in Fig. 7*B* is not linear, which supports the conclusion that this calcium channel is better represented by a permeability than a conductance (Hagiwara and Byerly, 1981).

For calcium tail currents recorded at −60 mV, two exponential components (2.58 ± 0.39 and 0.56 ± 0.22 ms, n = 8) were clearly necessary to describe the time course accurately. No differences in the time constants were observed for different initial voltage levels for repolarizations to −60 mV. The voltage dependence of the two time constants for the turn-off of I_{Ca} is illustrated in Fig. 8. Calcium tail currents to different voltage levels from a pulse to 24 mV were fitted with the sum of two exponentials and the resultant time constants were plotted against the postpulse level (Fig. 8*A*). The fast time constant appears to be voltage independent, whereas the slower time constant is strongly influenced by voltage (Fig. 8*B*). Fenwick et al. (1982) reported a similar voltage-independent

fast time constant and voltage-dependent slow time constant for Ca tail currents in adrenal chromaffin cells. The limited frequency response of our recording system, however, precluded an absolute determination of the exact voltage dependence of the fast component.

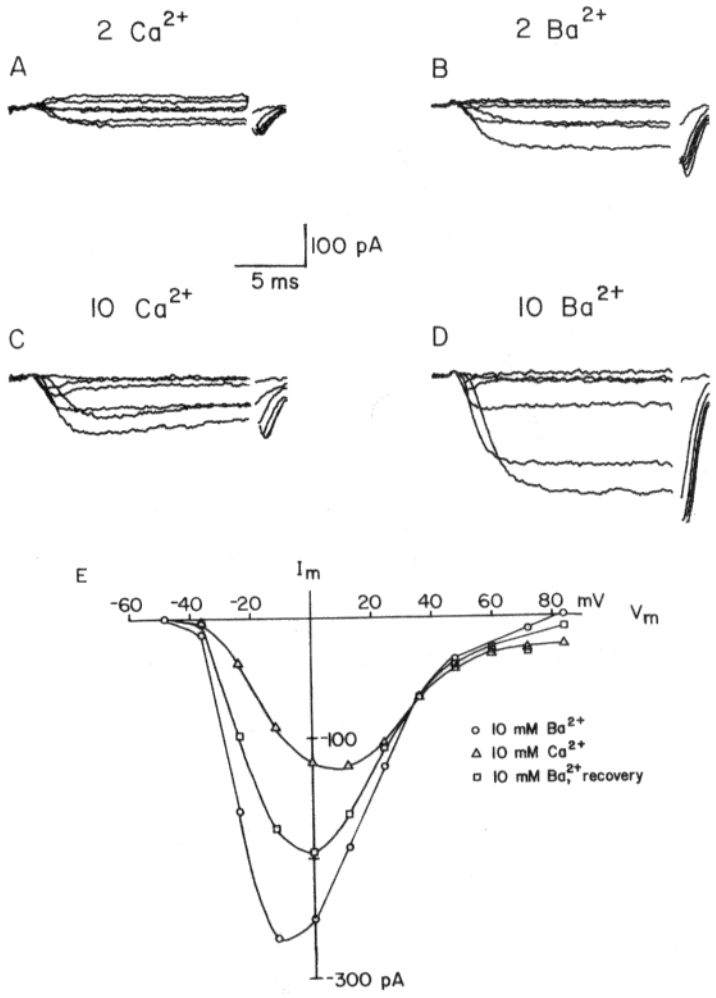

FIGURE 6. Ionic currents through Ca^{2+} channels in GH3 cells. Records obtained for voltage steps to −36, −12, 12, 36, 60, and 84 mV from a V_H of −60 mV. Internal solution (mM): 170 mM NMG aspartate, 2 ATP, 0.3 cAMP, 2 EGTA, 25 glucose, and 5 Hepes. (*A*) Calcium currents in cell 4/21/82-1. External solution (mM): 150 NaCl, 2 $CaCl_2$, 20 glucose, 5 Hepes, and 3×10^{-7} M TTX. (*B*) Barium currents, same cell as in *A*, where 2 mM $BaCl_2$ replaced $CaCl_2$ in the external solution. (*C*) Calcium currents in cell 4/21/82-6. External solution (mM): 150 NaCl, 10 $CaCl_2$, 10 glucose, 5 Hepes, and 3×10^{-7} M TTX. (*D*) Barium currents recorded in the same cell as in *C* where 10 mM Ca^{2+} was replaced by 10 mM Ba^{2+}. (*E*) Current-voltage relationships for cell 4/21/82-6 in 10 mM Ba^{2+} (circles), 10 mM Ca^{2+} (triangles), and recovery in 10 mM Ba^{2+} (squares).

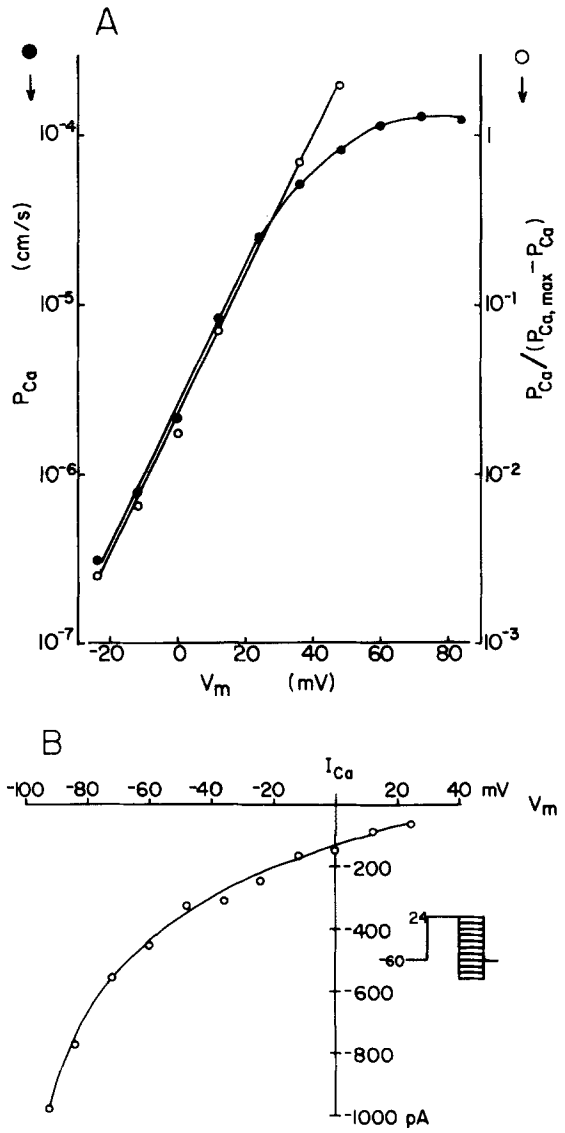

FIGURE 7. Calcium channels in GH3 cells are not ohmic. (*A*) Calcium permeability-voltage relationship. Permeability values were computed according to the Goldman-Hodgkin-Katz formulation and plotted as P (closed circles) and log $[P/(P_{max} - P)]$ (open circles) vs. membrane potential. GH3 cells 10/6/82-1. Internal solution (mM): 150 Cs^+, 130 aspartate$^-$, 20 Cl^-, 20 glucose, and 10 Hepes. External solution was the same as in Fig. 6*C*. (*B*) Calcium instantaneous current-voltage relationship. Current measured as described in text. Internal solution was the same as in *A*. External solution (mM): 136 TEA^+, 14 Cs^+, 130 aspartate$^-$, 10 $CaCl_2$, 10 glucose, 5 Hepes, and 3×10^{-2} M TTX. GH4 cell 2/28/83-5.

In practically all cells in which Ca or Ba tail currents were examined, both fast and slow components could be identified. However, the relative amplitude of the two components varied. In external tetraethylammonium (TEA)-saline (Fig. 9*D*), Ca tail currents typically exhibit a very small slow component; however, larger-amplitude slow tail components were occasionally observed. Small-amplitude slow components were only sometimes observed in external Na solutions.

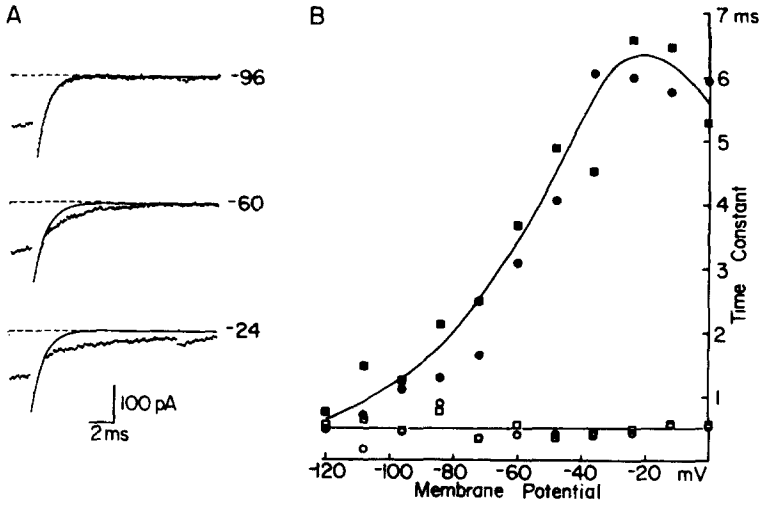

FIGURE 8. Voltage dependence of calcium tail current deactivation. (*A*) Examples of calcium tail currents (data points) recorded at the indicated voltages following a prepulse to +24 mV. The inward currents during the last 2 ms of each prepulse are also shown in each record. Single exponentials fit to the early time points of each record reveal the development of a second slower kinetic component in the tail currents for increasingly positive membrane potentials. GH3 cell 10/6/82-5. External solution was the same as in Fig. 6*C*. Internal solution was the same as in Fig. 7*A*. (*B*) Voltage dependence of calcium channel deactivation rates. Time constants were extracted from tail currents by fitting the slowest component, "peeling" the fit from the data, and fitting the remaining fast current component. The fast time constants (open symbols) were almost independent of membrane potential, while the slow time constants (filled symbols) were steeply voltage dependent. Each data point represents the mean of two determinations from each of two GH3 cells: 10/6/82-5 (circles) and 10/15/82-5 (squares). The external solution for cell 10/15/82-5 was normal solution with 3×10^{-7} M TTX. Internal solution was the same as in Fig. 7*A*.

Byerly and Hagiwara (1982) argue that in *Limnea* neurons the slowest component of their measured Ca tail currents is not a true Ca current since its amplitude increased with increasing duration pulses and since it increased in amplitude as the Ca current spontaneously diminished. In GH cells under the ionic conditions described above, Ca tail current amplitudes and time courses remained constant after pulses of increasing duration. Both slow and fast components of the Ca and Ba tail currents decrease in parallel with the rundown of the currents during the

depolarizing step. From these observations, it appears that the slow component of the tail currents is a true Ca current. However, further experiments are necessary to investigate a possible TEA sensitivity of the slow component.

Maximum barium current density was calculated from tail current measurements repolarizing to −60 mV after 4-ms pulses to 60 mV. The initial amplitude of the tail current was estimated by extrapolating an exponential fit to the early points of the tail current to the pulse offset. With 10 mM Ba^{2+} present externally, barium tail current amplitudes ranged from 242 pA in a 13-μm cell to 1,900 pA in a 15-μm cell. If the average Ba^{2+} current through a single calcium channel is assumed to be 0.2 pA (Hagiwara and Ohmori, 1982), the number of Ca channels can be calculated to be 1,210–9,500 per cell. If Ca channels are evenly distributed over a spherical cell, this value represents a density of 2.3–13.4 channels/μm^2.

A characteristic of this calcium current is an apparent slow decline during a depolarizing voltage step, which is more prominent in some cells than in others. Barium currents typically exhibit less decline than calcium currents. Before categorizing this decline as "inactivation" of the inward divalent channel, it was necessary to consider the alternative possibility that the decline represented the superposition of an outward ionic current unblocked by the internal cation

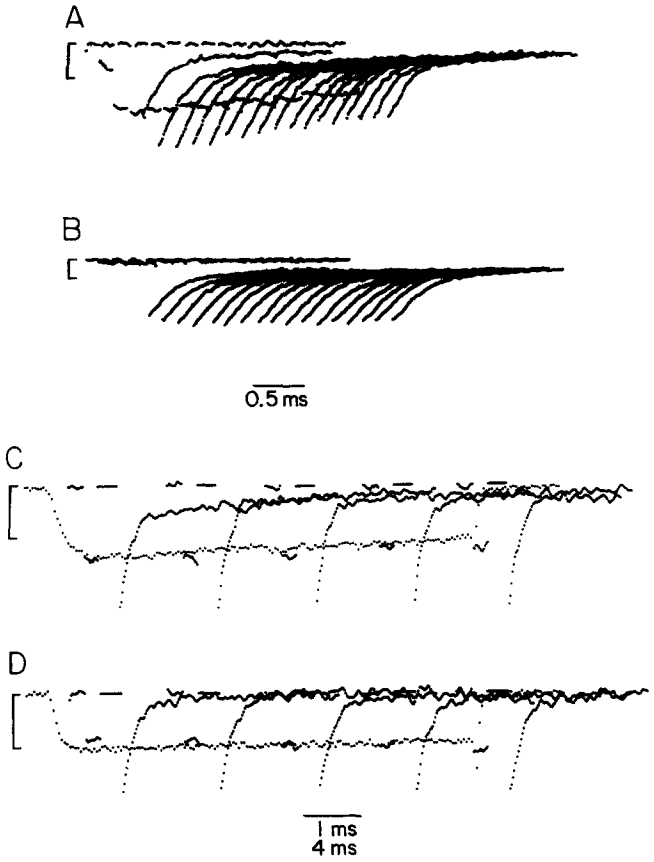

chosen to eliminate outward currents. To distinguish a true inactivation of calcium channels from the appearance of an opposing outward current, the tail current responses to the termination of applied voltage steps of increasing durations were examined. K^+ was excluded from both intra- and extracellular solutions. Both I_{Ca} during a step to 24 mV and the peak calcium tail current envelope for pulses of increasing duration decline prominently with Na^+ and Ca^{2+} present externally and Cs^+ internally (Fig. 9*A*). Addition of 11 mM EGTA to the internal solution failed to remove any of this apparent inactivation at 24 mV. The tail current envelope does not appear to decline, however, for a voltage step to 72 mV, where no I_{Ca} is apparent during the depolarizing voltage step (Fig. 9*B*). Barium tail current envelopes recorded in similar solutions do not decline with increasing pulse duration. Tail current amplitude under these ionic conditions may thus reflect an outward current component as well as an inward Ca^{2+} current component.

To clearly distinguish tail currents carried exclusively by Ca^{2+} from the contributions of other ions, the internal and external concentrations of Cl^- and Cs^+ were adjusted such that their equilibrium potentials were at the holding potential, −60 mV, where tail currents were measured. Under these conditions, the initial amplitude of the calcium tail current following a voltage step should be proportional to the calcium permeability at the end of the voltage step. If the calcium channels inactivate over time, the tail currents following increasingly longer voltage steps should decrease in amplitude. If, on the other hand, the calcium permeability remains constant and an opposing outward current acti-

---

FIGURE 9 (*opposite*). Calcium tail current envelopes suggest the presence of a superimposed outward current in Cs^+-dialyzed cells. Tail currents were recorded (20-μs sampling interval) at −60 mV following Ca channel-activating prepulses of progressively increasing duration. In *A* and *B*, the data shown are the baseline current prior to the prepulse, the last segment of inward calcium current before the tail, and the tail current. Successive records have been translated along the time axis by an arbitrary amount. In *C* and *D*, the Ca current during a 32-ms pulse is shown (longer time scale) with superimposed tail currents (shorter time scale) translated along the time axis by an amount equal to the prepulse duration at the longer time scale. (*A*) Ca tail currents where $E_{Cs} = -\infty$ and $E_{Cl} = -52$ mV. Note that the prepulse current and tail envelope decay with similar time courses. GH3 cell 10/16/82-3 with a prepulse to +24 mV. External and internal solutions were as in Figs. 6*C* and 7*A*, respectively. (*B*) Same cell as in *A*, with a voltage prepulse to +72 mV. (*C*) Ca tail currents with E_{Cs} and E_{Cl} adjusted to equal −60 mV. Note that although the prepulse current declines, the tail current envelope does not. GH4 cell 3/17/83-4 following prepulses to +24 mV of 2, 10, 18, 26, and 34 ms duration. Solutions: external (mM): 130 Na^+, 10 Ca^{2+}, 14 Cs^+, 150 Cl^-, 14 aspartate$^-$, 10 glucose, 5 Hepes, and 3×10^{-4} TTX; internal (mM): 150 Cs^+, 136 aspartate$^-$, 14 Cl^-, 10 glucose, and 5 Hepes. (*D*) Tail currents in the presence of external TEA^+ with E_{Cs} and $E_{Cl} = -60$ mV. Note the lack of decay in either prepulse current or tail envelope. GH4 cell 2/28/83-3. The external solution contained (mM): 136 TEA^+, 14 Cs^+, 10 Ca^{2+}, 150 Cl^-, 20 aspartate$^-$, 40 glucose, 10 Hepes, and 3×10^{-7} TTX. The internal solution was identical to *C*.

vates, the tail current amplitudes should remain constant for increasing pulse durations under these ionic conditions. The results of such an experiment are shown in Fig. 9*C* for a pulse to +24 mV, which is well within the voltage region to maximally activate calcium channels. The calcium current during the voltage step declines while the tail current envelope remains unchanged, which suggests that an opposing outward current is present during the step. To test whether this outward current was possibly carried by Cl^- or Cs^+, the equilibrium potential for Cl^- (E_{Cl}) was shifted away from the holding potential by replacement of external Cl^- with aspartate. When E_{Cl} was moved to 0 mV, the calcium tail currents remained unchanged with increased duration pulses (records not shown). Also, addition of 2 mM 4-AP externally failed to prevent the decline seen in I_{Ca} at +24 mV. When all the external Na^+ was replaced with TEA^+, neither I_{Ca} nor the tail current envelope showed any decline with increasing pulse duration (Fig. 9*D*). We conclude from these experiments that the decline of I_{Ca} with time in GH cells primarily reflects the activation of an outward current carried by Cs^+, which is blocked by extracellular TEA, and that calcium channels inactivate only slightly, if at all, in this time scale.

PROPORTIONS OF I_{NA} AND I_{CA} IN THE TWO CELL LINES The calcium current in GH4 cells is similar to that in GH3 cells in activation, inactivation, and pharmacological sensitivity. The peak density of I_{Ca} measured in 2 or 10 mM Ca or 10 mM Ba was comparable in both cell lines. This is noteworthy since the GH4 cells exhibited very little of the TTX-sensitive fast inward current. To compare the relative amount of sodium and calcium currents in the two cell lines, the sum of inward current at 2.2 ms (principally I_{Na}) and at 5.0 ms (principally I_{Ca}) after a voltage step to 0 mV was measured before and after TTX application. The ratio of this sum after TTX to that before TTX estimates the relative proportions of the inward current attributable to calcium in the two cell lines. For cells with only I_{Na}, the ratio should be zero. For cells exhibiting only I_{Ca}, the ratio should be 1.0. For GH3 cells, the ratio is 0.24 ± 0.16 ($n = 14$), which suggests that a large amount of the inward current is carried by sodium. In GH4 cells, the ratio is 0.83 ± 0.18 ($n = 11$), which suggests that practically all the inward current in these cells is attributable to calcium channels. A distinct I_{Na} was observed in only 2 out of 11 GH4 cells examined. In the other GH4 cells, deviations from 1.0 were visibly a result of I_{Ca} rundown and were not due to a separate I_{Na}.

Outward Ionic Currents

Outward current in GH3 and GH4 cells was studied with potassium as the sole intracellular cation and with TTX present externally to block sodium currents. When examined with fast sampling rates for short voltage steps, the outward currents turned on with a sigmoidal rise. Longer pulses revealed wide variations in the time courses. Fig. 10, *A* and *B*, illustrates examples of different cells whose outward currents partially inactivate or continue to rise slowly during the pulses. The cell in Fig. 10*C* exhibits outward currents which contain both inactivating and slowly rising components. It is impossible to distinguish these components in the cell of Fig. 10*D*, where the currents remain steady in time. No correlation

was observed between cell appearance, passive membrane properties or culture conditions, and the presence of any of these kinetic types. A correlation was found between outward current patterns and cell line. The inactivating outward current was observed more prominently in GH3 cells, while the slowly rising outward current was more frequently associated with GH4 cells (see Table II and subsequent discussion).

Only the inactivating outward current was always observed in extracellular solutions containing cobalt or cadmium. Either 25 mM TEA-bromide or 2 mM 4-AP applied externally blocked a large proportion of the outward currents.

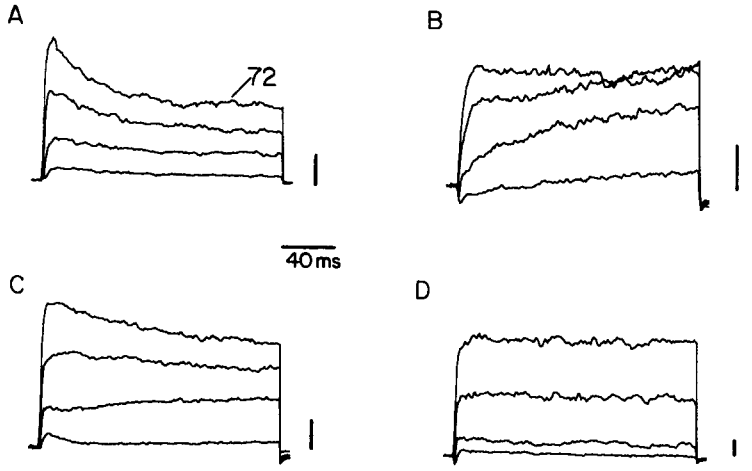

FIGURE 10. Examples of multicomponent outward currents in GH cells recorded for voltage pulses to 0, 24, 48, and 72 mV from a $V_H = -60$ mV. (*A*) Inactivating outward currents. GH4 cell 5/28/82-4. External solution (mM): 140 NaCl, 5 KCl, 10 $CaCl_2$, 5 Hepes, 10 glucose, and 3×10^{-4} TTX. Internal solution (mM): 150 K-aspartate, 30 glucose, and 5 Hepes. (*B*) Slowly rising outward currents. GH4 cell 9/14/82-4. Normal internal solution and normal external solution with TTX. (*C*) Outward currents with combined inactivating and slowly rising components. GH4 cell 9/20/82-3. Solutions were the same as in *B*. (*D*) Outward currents with indistinguishable kinetic components. GH3 cell 11/19/82-3. The external solution was the same as in *B*. Internal solution (mM): 150 K^+, 120 $aspartate^-$, 30 Cl^-, 10^{-6} M Ca buffered with EGTA, and 3×10^{-4} TTX. Vertical scale represents 200 pA in all cases.

Preliminary experiments were performed in eight cells using these compounds to test a possible pharmacological method of separating these current components. No consistent differential sensitivity to either TEA or 4-AP was found; therefore, further attempts at separation of the outward currents using these agents were not pursued.

These outward currents could reflect either an outward flux of potassium ions or an inward flux of chloride ions. To test for a possible chloride current, aspartate substitutions were performed both intra- and extracellularly. Both inactivating and slowly rising currents were observed in the aspartate solutions

TABLE II

Relative Amounts of $I_K(V)$ and $I_K(Ca)$

	GH3	GH4
Predominantly inactivating $I_K(V)$	51.5%	5.7%
Predominantly slow-rising $I_K(Ca)$	3.0%	34.4%
Equal amounts of both or undistinguishable	45.5%	60.0%
	33	35

(Fig. 11). No detectable difference was observed in the outward currents in the absence of chloride. Thus, we concluded that potassium is the major current carrier for these outward currents.

VOLTAGE-DEPENDENT POTASSIUM CHANNELS The peak current-voltage relationship for the inactivating component of outward current is illustrated in Fig. 12*A*. Cobalt was present in the bath to block I_{Ca} and any subsequent Ca-activated currents. This current activates at voltages above −24 mV and its amplitude increases monotonically with increasing voltage. Similar current-voltage curves were obtained in the absence of Co^{2+}, where extracellular Ca^{2+} was buffered to 10^{-8} M with EGTA. The voltage dependence of the inactivating outward current was identical for both cell lines. From the characteristic current-voltage relationship and the lack of sensitivity to external calcium ion or its blockers, the inactivating outward current was identified as passing through the delayed rectifier or voltage-dependent potassium channel, $I_K(V)$.

The inactivating outward currents decreased continuously during 185-ms pulses, rarely reaching a steady state level. In many cells this decline was exponential, but in some it appeared nearly linear. In two cells with extracellular Ca^{2+} buffered to 10^{-8} M, single exponentials were fit to the decay phase of $I_K(V)$. The time constants ranged from 20 to 80 ms, the longer values corresponding to larger depolarizations. The wide variation in apparent inactivation time course seen for all experiments may reflect overlapping activation of the slowly rising outward current.

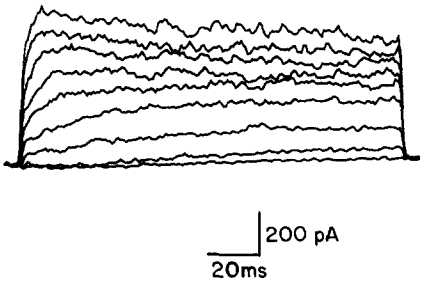

FIGURE 11. Chloride ion movement does not contribute significantly to recorded outward currents. Outward currents measured in the absence of either internal or external Cl^- for voltage pulses from −12 to +84 mV in 12-mV increments. The holding potential was −60 mV. GH4 cell 9/23/82-3. External solution (mM): 150 Na^+, 5 K^+, 2 Ca^{2+}, 159 aspartate$^-$, 1.3 $MgSO_4$, 10 Hepes, 30 glucose, and 3×10^{-4} TTX. The internal solution was the same as in Fig. 10*A*.

The voltage dependence of outward current inactivation was studied using a double-pulse protocol with extracellular calcium buffered to 10^{-8} M. The voltage of the prepulse was varied and the amplitude of outward current in response to

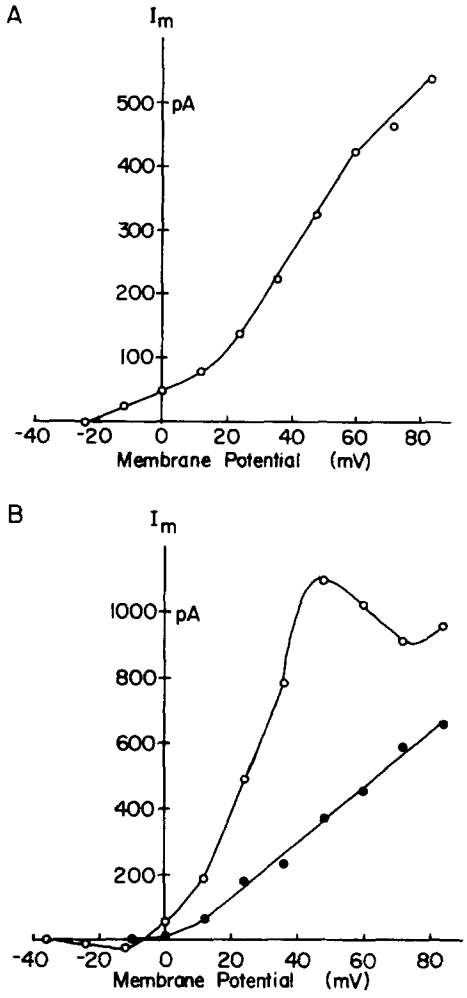

FIGURE 12. Current-voltage relationships for outward currents in GH cells. (*A*) Inactivating outward current. Data points obtained at peak outward current for indicated potentials. GH3 cell 4/30/82-7. External solution (mM): 150 NaCl, 5 KCl, 2 $CaCl_2$, 1.3 $MgCl_2$, 1 $CoCl_2$, 5 Hepes, 10 glucose, and 3×10^{-4} TTX. Internal solution (mM): 150 K-aspartate, 2 EGTA, 40 glucose, and 5 Hepes. (*B*) Slowly rising outward current. Data points represent current measured isochronally at 185 ms in normal external solution with 3×10^{-7} M TTX (open circles) and after (closed circles) addition of 0.6 mM $CdCl_2$. Normal internal solution. GH3 cell 1/21/83-1.

a 60-mV test pulse was monitored. The current from the test pulse was normalized with respect to the current without a prepulse and plotted vs. the prepulse potential in Fig. 13. Approximately 30% of the current is resistant to the

inactivation process. The voltage for half-maximal inactivation of the prepulse-sensitive current ($V_{0.5}$) is -36.8 ± 3.1 mV ($n = 5$, pooled GH3 and GH4 data). The inactivation of GH4 cells appeared to exhibit a less steep dependence on voltage than GH3 cells, but values for $V_{0.5}$ were comparable.

The inactivating property of this outward current channel is the basis for a "use-dependent" decrease in outward current seen with repeated pulses (inset of Fig. 13). When the time between a pair of 185-ms voltage pulses to +40 mV was varied, the amplitude of the outward current during the second pulse decreased for interpulse intervals up to 50 ms. This cumulative component of inactivation

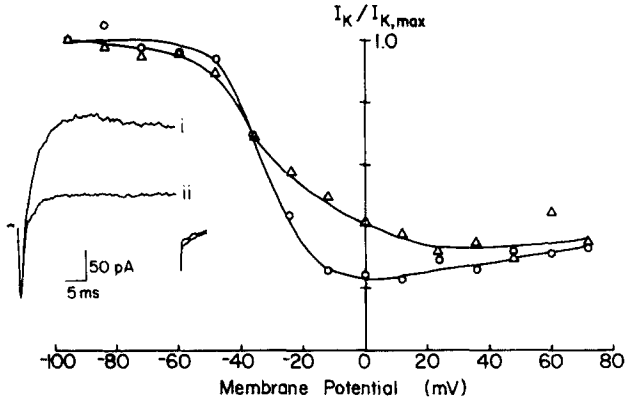

FIGURE 13. Inactivation of the delayed rectifier in GH cells. Steady state voltage dependence of $I_K(V)$ inactivation. Currents recorded at a test potential of +40 mV preceded by a 3-s prepulse to the potential indicated on the abscissa. A "gap" of 2 ms at the holding potential separated the conditioning and test pulses. Data points represent normalized (to maximum) currents for GH3 cell 9/21/82-2 (circles) and GH4 cell 9/21/82-5 (triangles). External solution (mM): 135 NaCl, 20 KCl, 5 $MgCl_2$, 10^{-8} M Ca^{2+} buffered with EGTA, 5 Hepes, and 10 glucose. Normal internal solution. An example of "use-dependent" outward current reduction caused by inactivation is shown in the inset as inward and outward current responses to an initial voltage step to +9 mV (*i*) and to the last of a rapid succession of such pulses (*ii*). Note the marked reduction in outward K current, but not inward Na current. GH3 cell 2/8/82-4 in normal external solution and dialyzed with the same internal solution as Fig. 12*A*.

is reminiscent of observations on inactivation in delayed rectifier channels in molluscan neurons (Aldrich et al., 1979). For interpulse intervals of >50 ms, the current amplitude during the second pulse recovered slowly with a time constant of 1.76 ± 1.12 s ($n = 7$, pooled GH3 and GH4 data). Recovery was 95% complete by 3 s. Recovery for interpulse intervals beyond 3 s was not examined and may have been even slower; thus, a second time constant for recovery from inactivation cannot be ruled out. Because of this long recovery period, individual voltage pulses for all outward current protocols except those involving intracellular calcium loading (see below) were delivered at rates of 2–4/min.

CALCIUM-ACTIVATED POTASSIUM CHANNELS In the majority of both GH3

and GH4 cells, the current-voltage curve is linear for voltages above 10 mV for outward currents measured at the peak or isochronally at 185 ms after a voltage step (Fig. 12*A*). However, in a few cells with a prominent slowly rising outward current, the isochronal current-voltage curve displays a "negative conductance" region at high voltages (Fig. 12*B*, open circles). This N-shape is a characteristic of calcium-activated potassium currents in molluscan neurons, where the decrease in current amplitude is due to a decrease in calcium influx as the voltage approaches E_{Ca} (Meech and Standen, 1975). Correspondingly, when 0.6 mM Cd^{2+} was added to the bath to block I_{Ca}, the slowly rising outward current disappeared, and the isochronal outward current-voltage curve lost the N-shaped component (Fig. 12*B*, filled circles). These observations suggest that the slowly rising outward current is a calcium-activated potassium current, $I_K(Ca)$. No differences were observed in the voltage dependence of the N-shaped *I-V* relationships between the two cell lines.

Because the slow activation of $I_K(Ca)$ and the inactivation of the delayed rectifier current often displayed similar voltage dependences and time courses, it was possible that in some cells neither of these currents could be clearly distinguished from the other (e.g., Fig. 10, *C* and *D*). These two potassium currents could, for example, sum to produce an outward current that turns on sigmoidally and remains approximately constant for the duration of the experimental pulse. It was of interest, therefore, to try to discriminate both types of potassium current in the same cell. A way was sought to uncover a slowly rising current in a cell which initially displayed only prominent inactivation.

To do this, a prepulse protocol was designed to elevate the internal calcium concentration to maximize any Ca-dependent currents. A prepulse voltage (−12 mV) was chosen near the peak of the calcium *I-V* relationship (Fig. 6*E*). A prepulse to −12 mV also served nicely to induce a voltage-dependent inactivation of the delayed rectifier current as previously described (Fig. 13). Outward currents recorded after this prepulse showed a marked increase in amplitude and a distinct change of the time course from inactivating to slowly rising (Fig. 14, *A* and *B*). The addition of cadmium or cobalt to the bath reduced overall outward current amplitude and the prepulse protocol failed to elicit the slowly rising current. Only the inactivating outward current, $I_K(V)$, remained (Fig. 14*C*). In a cell initially displaying only the slowly rising current, cadmium caused a reduction in current amplitude and the appearance of the inactivating current. In several calcium-loaded cells, $I_K(Ca)$ during the test pulse did not exhibit the slowly rising activation; instead, it turned on rapidly after the onset of a voltage step (Fig. 10*D*). This suggests that the slow onset seen under normal conditions results from the time course of entry and accumulation of intracellular calcium.

The voltage dependence of $I_K(Ca)$ was examined by varying the prepulse voltage and measuring peak current. These values were normalized relative to those measured following the most negative prepulse. This experiment was performed in the presence of 2 mM Ca^{2+} externally (Fig. 15, open circles) and subsequently with Ca^{2+} buffered to 10^{-8} M with EGTA (Fig. 15, closed circles). The normalized current values in the absence of Ca^{2+} were subtracted from those in the presence of Ca^{2+}. The resulting difference current-voltage curve

(dashed line) represents the net macroscopic voltage dependence of I_K(Ca). This voltage dependence clearly parallels that for I_{Ca} (Fig. 15*B*), as is expected for a current whose activation is dependent on Ca^{2+} entry.

PROPORTIONS OF VOLTAGE-ACTIVATED AND CA^{2+}-ACTIVATED K CHANNELS IN THE TWO CELL LINES As previously noted, GH3 and GH4 cells exhibit differing proportions of the voltage-dependent and calcium-activated potassium currents. All cells in which outward currents were studied were classified according to the overwhelming prevalence of $I_K(V)$ or I_K(Ca) or the inability to clearly distinguish between the two classes (Table II). From this classification, the delayed rectifier is more prominent in GH3 cells, whereas I_K(Ca) is more readily seen in GH4 cells. About half the cells from both cell lines displayed outward currents

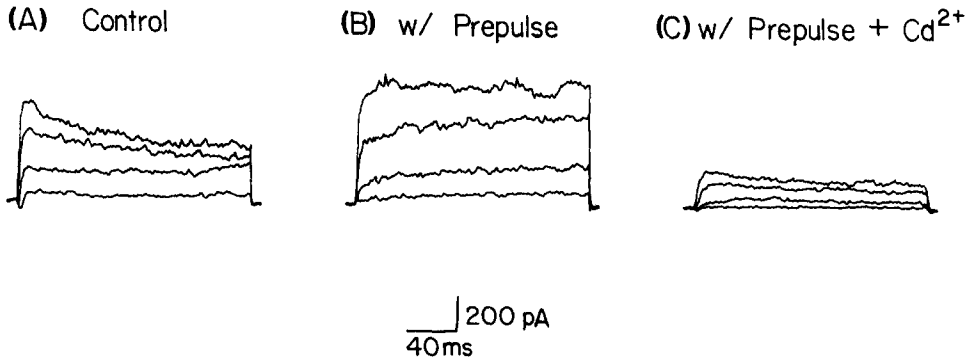

FIGURE 14. Accentuation of slowly rising outward current component by treatments which elevate intracellular Ca^{2+}. (*A*) Predominantly inactivating outward currents for single voltage pulses to 0, 24, 48, and 72 mV from a V_H = −60 mV. (*B*) Currents from the same cell at the same voltages preceded by a 1-s conditioning voltage step to −12 mV and a "gap" of 10 ms. Note the increased amplitude and slowly activating nature of the currents. (*C*) Currents obtained with the same prepulse-test pulse sequence as in *B* following the addition of 1 mM $CdCl_2$ to the external bath. GH3 cell 9/16/82-6. Normal external solution with 3×10^{-7} M TTX. Normal internal solution.

that appeared to be a mixture of both I_K(Ca) and $I_K(V)$. An attempt was made to compare current densities for these two K components from cells where data had been collected for both single voltage steps and voltage steps with prepulses to −12 mV. The peak current for a single voltage pulse to +48 mV was taken as a measure of $I_K(V)$. The current at 185 ms in response to the double-pulse protocol (V_1 = −12 mV, V_2 = +48 mV) was considered to represent the current attributable to I_K(Ca). Currents were normalized according to membrane surface area and averaged. The averaged current density for $I_K(V)$ in GH3 cells (1.12 ± 0.29 pA/μm^2, n = 11) was significantly greater than for GH4 cells (0.80 ± 0.13 pA/μm^2, n = 5; $P < 0.05$). I_K(Ca) average current density was not significantly different between the two cell lines (0.84 ± 0.38 pA/μm^2, n = 11 in GH3 cells; 1.02 ± 0.36 pA/μm^2, n = 5 in GH4 cells).

DISCUSSION

These data demonstrate that the GH3 and GH4 cells possess voltage-activated calcium channels, voltage-activated potassium channels, and calcium-activated potassium channels. In addition, GH3 cells possess voltage-dependent sodium channels. In general, these currents behave similarly to those found in other excitable membranes.

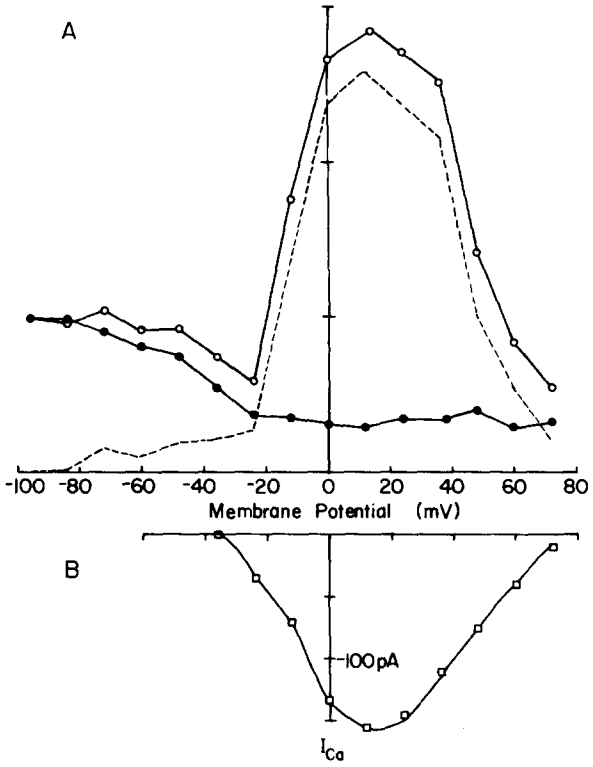

FIGURE 15. Apparent voltage dependence of I_K(Ca) follows that of I_{Ca}. Outward ionic currents were recorded at +40 mV using the protocol described in Fig. 13. The responses were normalized to that seen with a prepulse to −96 mV and are plotted in *A* vs. prepulse voltage for two conditions: 2 mM Ca^{2+} in the external solution (open circles) and with external Ca^{2+} buffered to 10^{-8} M with EGTA (filled circles). As the conditioning potential becomes more positive, the "inactivation" seen in both Ca^{2+} concentrations gives way to a dramatic increase in current (2 mM Ca^{2+}), which again falls at potentials above +20 mV. The difference between the two sets of data is indicated by the dashed line, which is taken to represent the Ca^{2+}-activated K current component. GH3 cell 9/28/82-2 dialyzed with normal internal solution and an external solution containing (mM): 135 NaCl, 20 KCl, 5 Hepes, 10 glucose, and either 1.3 Mg^{2+}/2 Ca^{2+} or 5 Mg^{2+}/10^{-8} M Ca^{2+}. A typical calcium current-voltage relationship from a different cell is illustrated in *B* for comparison with the difference curve. GH3 cell 10/15/82-5 in the same solutions as for Fig. 8*B*.

The sodium current of GH3 cells is qualitatively similar to I_{Na} from neuroblastoma cells (Moolenaar and Spector, 1978), mammalian node of Ranvier (Chiu et al., 1979), and bovine adrenal chromaffin cells (Fenwick et al., 1982). This current rapidly activates and subsequently inactivates to a small steady state level. The voltage dependences of peak current and of the inactivation process are similar to those reported for adrenal chromaffin cells (Fenwick et al., 1982) and neuroblastoma cells (Moolenaar and Spector, 1978). Estimates of channel density calculated above indicate that GH3 cell membranes contain ~250–1,300 sodium channels per cell.

The absence of the sodium current in the GH4 subclone of the GH3 cell line is an intriguing observation. Both cell types secrete prolactin and, to a lesser extent, growth hormone under similar types of hormonal regulation (Dannies and Tashjian, 1973; our unpublished observations). Since the GH4 cells exhibit relatively little I_{Na}, cell membrane depolarization via sodium channel permeability changes must not be a requirement for hormone release.

The calcium current in both GH3 and GH4 cells has been identified on the basis of its time course, its sensitivity to divalent cation block, and the ability of Ba^{2+} to substitute for Ca^{2+} as current carrier. Our identification of $I_{Ca}(V)$ is consistent with a study of Ca^{2+} current in GH3 cells by Hagiwara and Ohmori (1982, 1983). In their study of single-channel Ca currents they suggested that there are two distinct processes in the activation of I_{Ca}. Our measurements of slow voltage-dependent and fast voltage-independent components in Ca tail currents agree with their determination of two time constants for the closed time histograms (Hagiwara and Ohmori, 1983). Our data represent an improvement over their original measurements of only a single component in Ca tail currents (Hagiwara and Ohmori, 1982). Similar kinetic components have been reported for Ca currents in adrenal chromaffin cells (Fenwick et al., 1982).

At large positive depolarizations, small outward currents are sometimes detected under ionic conditions where only inward Ca^{2+} current is expected. These outward currents could reflect a true reversal of current through the Ca channel or an additional unblocked outward current. Lee and Tsien (1982) and Fenwick et al. (1982) have suggested that, under similar circumstances in heart cells and adrenal chromaffin cells, respectively, internal K^+ or Cs^+ are flowing outward through the Ca channel. In a small number of GH cells, the activation kinetics of these outward currents were consistent with those expected for ion movement through Ca channels, and their current-voltage relationships were not linear in the voltage range near the apparent reversal potential, in agreement with the observations made by Fenwick et al. (1982). In such cases we may also have observed a true reversal of current through Ca channels.

In the majority of cells exhibiting a reversal potential, however, the kinetics of the outward current resembled those of the potassium currents. Several lines of evidence lead us to believe that this outward current flows through potassium channels. (*a*) Currents at the apparent reversal potential were often inward initially and became outward by the end of the pulse, which is similar to findings in *Limnea* reported by Byerly and Hagiwara (1982). This is in contrast to the total absence of current at the Ca reversal potential in heart cells (Lee and Tsien,

1982). (*b*) In the majority of GH cells these outward currents did not exhibit spontaneous rundown as did I_{Ca}. (*c*) Co^{2+}, at concentrations used to block inward Ca currents, failed to remove the outward currents at high voltages. (*d*) These outward currents persist in the absence of chloride both externally and internally, which eliminates the possibility that they represent an undetected inward Cl^- flux. (*e*) Under conditions in which Ba ions carried the current through the calcium channels, the opposing outward current component was not observed. Ba ions have been shown to block voltage-activated K channels in a variety of preparations (Hagiwara et al., 1974; Gorman and Hermann, 1979; Armstrong and Taylor, 1980; Eaton and Brodwick, 1980; and our unpublished observations). Ba^{2+} is also much less effective than Ca^{2+} in activating the Ca-activated K conductance (Gorman and Hermann, 1979).

In these cells the possibility remains that Cs^+ or NMG^+ (the latter almost totally impermeant through delayed rectifier K channels in squid axon [Oxford and Adams, 1981]) do not completely block K channels at these very depolarized voltages. Rather, they may be driven through the channels by the large driving force. Such behavior has been reported for sodium flux through K channels in squid axon (French and Wells, 1977). The measured Cs^+ permeability relative to K^+, through the delayed rectifier channel, ranges from 0.077 in frog node (Hille, 1973) to 0.18 in *Helix* neurons (Reuter and Stevens, 1980). In GH cells, $I_K(V)$ at 60 mV typically has a peak value of 600 pA. Assuming that the channels obey the constant field equation (Goldman, 1943; Hodgkin and Katz, 1949) and using the permeability ratios given above, Cs^+ could be expected to carry 46–100 pA of outward current at this voltage under our recording conditions. These values are consistent with the amplitudes of outward current we observed during I_{Ca} measurements.

Current flow through the Ca-activated K channels may also contribute to the observed outward currents. Gorman et al. (1982) reported that the Ca-activated K channel in *Aplysia* is extremely selective, having a relative permeability for Cs of 0.03. Using similar assumptions as stated above, Cs could be expected to carry a maximum of 18 pA of current. We have observed that these outward currents occur in cells where 2 mM EGTA and 0 Ca have been included in the pipette internal solution. However, we have no independent measure of intracellular Ca^{2+} activity and cannot be sure that it was effectively buffered to a sufficiently low level to prevent channel activation. We cannot rule out the additional possibility that this outward flux of Cs ions might flow through calcium-activated nonspecific cation channels recently reported in heart cells and neuroblastoma (Colquhoun et al., 1981; Yellen, 1982). The apparent lack of selectivity of this channel would allow it to pass many and perhaps all of the cations we employed with an apparent reversal potential near 0 mV.

Such outward currents also contribute to I_{Ca} recordings at lower voltages, conferring upon them the semblance of inactivation. This apparent inactivation occurs quite regularly under normal recording conditions. Only when Ca^{2+} tail currents were studied under conditions of controlled Cs^+ reversal potential was the presence of the outward conductance detected. We cannot clearly identify the channel population through which the opposing Cs^+ current flows. Although

150 mM TEA^+ blocked this Cs^+ current, 2 mM 4-AP was not sufficient to prevent it. The failure to achieve a complete block might be attributable to the extremely large driving force on Cs^+ in these experiments.

The inactivating outward current observed in these cell lines is clearly a delayed rectifier and not an early transient current (I_A), as seen in molluscan neurons (Conner and Stevens, 1971; Thompson, 1977). The voltage dependence of inactivation reported in Fig. 13 occurs over a voltage range significantly more depolarized than that of I_A. I_A is totally inactivated at membrane potentials of −40 to −50 mV (Conner and Stevens, 1971), while the inactivating current in GH3 and GH4 cells is only 30% inactivated at −12 mV. The outward currents reported here do not activate at low membrane potentials and hyperpolarizing prepulses do not remove the inactivation, both characteristics of I_A (Adams et al., 1980). The inactivating outward current in GH3 and GH4 cells resembles the inactivating delayed rectifier seen in molluscan neurons and neuroblastoma cells (Aldrich et al., 1979; Moolenaar and Spector, 1978). While the time constants of onset and recovery from inactivation are smaller in these mammalian tumor cells than in molluscan neurons, the voltage dependences of inactivation are nearly identical (Aldrich et al., 1979). In both of these preparations, the delayed rectifier is approximately half-inactivated at resting membrane potentials, repeated depolarizing pulses produce a cumulative inactivation, and Co^{2+} and Cd^{2+} are ineffective in blocking this process (Adams et al., 1980). The extreme variability of the time course of inactivation of the delayed rectifier is consistent with observations in neuroblastoma cells reported by Moolenaar and Spector (1978).

The possibility that inactivation of $I_K(V)$ is attributable to accumulation of K ions at the external surface of the cell is not likely since prominent inactivating outward currents were observed with 5 or 20 mM K^+ in the external solution. In addition, only single isolated cells were recorded from in a continuously perfused bath. Electron microscopy reveals no membrane invaginations or external basement membrane which could serve to restrict the flow of solution around the cells and form a compartment where K ions could accumulate (Tixier-Vidal et al., 1975).

The appearance of a Ca^{2+}-activated K^+ conductance is not surprising given the reported observations of single Ca-sensitive K channel currents in adrenal chromaffin cells (Marty, 1981), in GH cells (G. Yellen, personal communication, and our unpublished observations), and in a mouse pituitary tumor line, AtT/20, (Wong et al., 1982). The slow activation of this outward current is similar to the I_K(Ca) reported in neuroblastoma (Moolenaar and Spector, 1979), in *Tritonia* (Thompson, 1977), in *Helix* (Lux and Hofmeier, 1982), and in the presynaptic terminal of squid giant synapse (Augustine and Eckert, 1982). This slowly activating current is observable only under conditions in which inward Ca currents are present or intracellular Ca^{2+} is elevated by prepulses or by Ca-EGTA buffers. It is not seen in cells dialyzed with intracellular EGTA or perfused externally with Co^{2+} or Cd^{2+}. In whole cells voltage-clamped for >20 min, in which Ca current has spontaneously declined, it is very difficult to elicit any slowly rising outward current.

The differential appearance of the outward currents probably represents a true difference in the channel density in the two cell lines. By examining the calculated outward current densities and the cell categorizations, it is apparent that $I_K(V)$ is more abundant in GH3 cells. $I_K(Ca)$, while more apparent in GH4 cells, may not reflect an actual increase in channel density over GH3 cells. Since the current density measurements were made at nonsaturating levels of $I_K(Ca)$, this comparison may not be totally reliable. The differential distribution of the outward currents does not reflect differences in their activation properties between the cell lines since the voltage dependences of $I_K(V)$ and $I_K(Ca)$, respectively, are identical in both cell lines. It is conceivable that the apparent calcium sensitivity of $I_K(Ca)$ may be greater in GH4 cells, thus resulting in a more prominent $I_K(Ca)$ component. Since the calcium current densities are approximately equivalent between the two cell lines, an enhanced Ca sensitivity in GH4 cells should be seen as a shift in the $I_K(Ca)$ vs. voltage curve to lower voltages. This is not observed. It is therefore not likely that differences in individual K channel properties exist between the two cell lines. Rather, the GH3 cells probably contain a higher density of delayed rectifier channels.

The proportions of the different types of inward or outward currents varied greatly from cell to cell within each cell line, even among cells from the same coverslip. Such variability occurred in addition to the consistent predominance of $I_K(V)$ and I_{Na} in GH3 cells and of $I_K(Ca)$ and I_{Ca} in GH4 cells. The only difference between the cell culture conditions of the two cell lines was the addition of 2.5% fetal calf serum to the GH3 medium. Control experiments to examine the possibility that the serum supplement was somehow related to the electrophysiological differences were performed. When fetal calf serum was added to the GH4 medium and not the GH3 medium, no change was observed in the characteristic distribution of current types displayed by either cell line. Such variability may be a general trait of these cell lines. Variations have been reported in their staining for antibodies to prolactin (Hoyt and Tashjian, 1980; J. M. Dubinsky and B. Beckman, unpublished observations). Additionally, plasticity has been observed in their responses to drugs, as they apparently lose sensitivity to some substances after years in culture (Dannies et al., 1977; P. S. Dannies, personal communication; Taraskevich and Douglas, 1980). This regularly observed variability could be due to the presence of different subpopulations of cells or to cells at different stages of the cell cycle. Alternatively, given the tumorigenic origin of the cell lines, plasticity may be a limitation of the preparation.

While no differences in the proportions of action potentials from these two cell lines have been reported, the differential appearance of these channel populations would predict that such differences may be detectable. GH3 cell action potentials should exhibit TTX sensitivity and a faster rate of rise than those in GH4 cells. GH4 action potentials should be longer in duration than those of GH3 cells since they have less $I_K(V)$ to repolarize the cell rapidly. If a predominance of I_{Ca} and $I_K(Ca)$ together underlies bursting behavior (Thompson and Aldrich, 1980; Gorman and Hermann, 1982), then GH4 cells might be expected to show a greater tendency to bursting or spontaneous activity than

GH3 cells. Indeed, Taraskevich and Douglas (1980) report the occurrence of bursts of action potentials but do not state whether the cell in question was a GH3 or a GH4.

Understanding the basis for electrical activity of GH cells is of importance since there is increasing evidence for the involvement of electrical activity in the hormone release process. The calcium hypothesis of excitation-secretion coupling (Douglas, 1968) postulates that Ca entry via voltage-dependent Ca channels is necessary for exocytosis of hormone. Consistent with this, agents that stimulate secretion also affect the electrical activity of GH3 and GH4 cells. Thyrotropin-releasing hormone increases the frequency of firing in GH3 cells (Kidokoro, 1975; Dufy et al., 1979*a*; Taraskevich and Douglas, 1980), prolongs the action potential duration (Sand et al., 1980; Kaczorowski et al., 1983), and causes a transient hyperpolarization and subsequent enhancement of spike generation (Ozawa and Kimura, 1979; Ozawa, 1981). While these authors suggest that these changes are attributable to alterations in the resting permeability to potassium, changes in active calcium and potassium conductances may also be involved (Kaczorowski et al., 1983). Spike threshold is a sensitive function of the interplay between activation and inactivation processes for all the populations of channels present. Alterations in the voltage dependence of these conductances or modulation of the number and/or single-channel conductances of these channels may account for the variations of firing frequency reported. It is hoped that the description of ionic currents presented here will provide a basis for future work focusing on the sites of action of the secretory agents which modulate electrical activity in GH cells.

The authors wish to thank Dr. Priscilla Dannies for providing the GH4/C1 subclone for study and Victoria Allgood for technical assistance in maintaining the cultures.
This study represents experiments performed in partial fulfillment of the requirements for the Ph.D. degree in Neurobiology at the University of North Carolina by J.M.D. This research was supported by the National Institutes of Health through grant NS-18788 and by National Institutes of Mental Health grant MH-14277.

Received for publication 5 April 1983 and in revised form 24 September 1983.

REFERENCES

Adams, D. J., S. J. Smith, and S. H. Thompson. 1980. Ionic currents in molluscan soma. *Annu. Rev. Neurosci.* 3:141–167.

Adler, M., B. S. Wong, S. L. Sabol, N. Busis, M. B. Jackson, and F. F. Weight. 1983. Action potentials and membrane ionic channels in clonal anterior pituitary cells. *Proc. Natl. Acad. Sci. USA.* 80:2086–2090.

Aldrich, R. W., Jr., P. A. Getting, and S. H. Thompson. 1979. Inactivation of delayed outward current in molluscan neurone somata. *J. Physiol. (Lond.).* 291:507–530.

Armstrong, C. M., and S. R. Taylor. 1980. Interaction of barium ions with potassium channels in squid giant axons. *Biophys. J.* 30:473–488.

Augustine, G., and R. Eckert. 1982. Two presynaptic potassium currents at the squid giant synapse. *Soc. Neurosci. Abstr.* 8:497. (Abstr.)

Biales, B., M. A. Dichter, and A. Tischler. 1977. Sodium and calcium action potentials in pituitary cells. *Nature (Lond.).* 267:172–174.

Byerly, S., and S. Hagiwara. 1982. Calcium currents in internally perfused nerve cell bodies of *Limnea stagnalis*. *J. Physiol. (Lond.)*. 322:503–528.

Chiu, S. Y., J. M. Ritchie, R. B. Rogart, and D. Stagg. 1979. A quantitative description of membrane currents in rabbit myelinated nerve. *J. Physiol. (Lond.)*. 292:149–166.

Conner, J. A., and C. F. Stevens. 1971. Voltage clamp studies of a transient outward membrane current in gastropod neural somata. *J. Physiol. (Lond.)*. 213:21–30.

Colquhoun, D., E. Neher, H. Reuter, and C. F. Stevens. 1981. Inward current in cultured cardiac cells. *Nature (Lond.)*. 294:752–754.

Dannies, P. S., and A. H. Tashjian, Jr. 1973. Effects of thyrotropin-releasing hormone and hydrocortisone on synthesis and degradation of prolactin in a rat pituitary cell strain. *J. Biol. Chem.* 248:6174–6179.

Dannies, P. S., P. M. Yen, and A. H. Tashjian, Jr. 1977. Anti-estrogenic compounds increase prolactin and growth hormone synthesis in clonal strains of rat pituitary cells. *Endocrinology*. 101:1151–1156.

Douglas, W. W. 1968. Stimulus-secreting coupling: the concept and clues from chromaffin and other cells. *Br. J. Pharmacol.* 34:451–474.

Dubinsky, J. M., and G. S. Oxford. 1982. Comparison of ionic currents in voltage-clamped pituitary tumor cells in culture. *Soc. Neurosci. Abstr.* 8:60. (Abstr.)

Dufy, B., and J. L. Barker. 1982. Calcium-activated and voltage-dependent potassium conductances in clonal pituitary cells. *Life Sci.* 30:1933–1941.

Dufy, B., J. D. Vincent, H. Fleury, P. duPasquier, D. Gourdji, and A. Tixier-Vidal. 1979*a*. Membrane effects of thyrotropin-releasing hormone and estrogen shown by intracellular recording from pituitary cells. *Science (Wash. DC)*. 204:509–511.

Dufy, B., J. D. Vincent, H. Fleury, P. duPasquier, D. Gourdji, and A. Tixier-Vidal. 1979*b*. Dopamine inhibition of action potentials in a prolactin secreting cell line is modulated by estrogen. *Nature (Lond.)*. 282:855–857.

Eaton, D. C., and M. S. Brodwick. 1980. Effects of barium on the potassium conductance of squid axon. *J. Gen. Physiol.* 75:727–750.

Fenwick, E. M., A. Marty, and E. Neher. 1982. Sodium and calcium channels in bovine chromaffin cells. *J. Physiol. (Lond.)*. 331:599–635.

French, R. J., and J. B. Wells. 1977. Sodium ions as blocking agents and charge carriers in the potassium channel of the squid axon. *J. Gen. Physiol.* 70:707–724.

Goldman, D. E. 1943. Potential, impedance and rectification in membranes. *J. Gen. Physiol.* 27:37–60.

Gorman, A. L. F., and A. Hermann. 1979. Internal effects of divalent cations in potassium permeability in molluscan neurons. *J. Physiol. (Lond.)*. 296:393–410.

Gorman, A. L. F., and A. Hermann. 1982. Quantitative differences in the currents of bursting and beating pace-maker neurones. *J. Physiol. (Lond.)*. 333:681–699.

Gorman, A. L. F., J. C. Woolum, and M. C. Cornwall. 1982. Selectivity of the Ca^{++}-activated and light-dependent K^+ channels for monovalent cations. *Biophys. J.* 38:319–322.

Hagiwara, S., and L. Byerly. 1981. Calcium channels. *Annu. Rev. Neurosci.* 4:69–125.

Hagiwara, S., J. Fukuda, and D. C. Eaton. 1974. Membrane currents carried by Ca, Sr, and Ba in barnacle muscle fibers during voltage clamp. *J. Gen. Physiol.* 63:564–578.

Hagiwara, S., and H. Ohmori. 1982. Studies of calcium channels in rat clonal pituitary cells with patch electrode voltage clamp. *J. Physiol. (Lond.)*. 331:231–252.

Hagiwara, S., and H. Ohmori. 1983. Studies of single calcium channel currents in rat clonal pituitary cells. *J. Physiol. (Lond.)*. 336:649–661.

Hamill, O. P., A. Marty, E. Neher, B. Sakmann, and F. J. Sigworth. 1981. Improved patch clamp techniques for high-resolution current recordings from cells and cell-free membrane patches. *Pflügers Arch. Eur. J. Physiol.* 391:85–100.

Hille, B. 1973. Potassium channels in myelinated nerve. Selective permeability to small cations. *J. Gen. Physiol.* 61:669–686.

Hodgkin, A. L., and B. Katz. 1949. The effect of sodium ions on the electrical activity of the giant axon of the squid. *J. Physiol. (Lond.).* 108:37–77.

Horn, R., J. Patlak, and C. F. Stevens. 1982. The effect of tetramethylammonium on single sodium channel currents. *Biophys. J.* 36:321–328.

Hoyt, R. F., and A. H. Tashjian, Jr. 1980. Immunocytochemical analysis of prolactin production by monolayer cultures of GH3 rat anterior pituitary tumor cells. II. Variation in prolactin content of individual cell colonies, and dynamics of stimulation with thyrotropin releasing hormone (TRH). *Anat. Rec.* 197:163–176.

Kaczorowski, G. J., R. L. Vandlen, G. M. Katz, and J. P. Reuben. 1983. Regulation of excitation-secretion coupling by thyrotropin-releasing hormone (TRH): evidence for TRH receptor-ion channel coupling in cultured pituitary cells. *J. Membr. Biol.* 71:109–118.

Kidokoro, Y. 1975. Spontaneous calcium action potentials in a clonal pituitary cell line and their relationship to prolactin secretion. *Nature (Lond.).* 258:741–742.

Lee, K. S., and R. W. Tsien. 1982. Reversal of current through calcium channels in dialysed single heart cells. *Nature (Lond.).* 297:498–501.

Lux, H. D., and G. Hofmeier. 1982. Properties of a calcium- and voltage-activated potassium current in *Heli pomatia* neurons. *Pflügers Arch. Eur. J. Physiol.* 394:61–69.

Marty, A. 1981. Ca-dependent K channels with large unitary conductance in chromaffin cell membranes. *Nature (Lond.).* 291:497–500.

Meech, R. W., and N. B. Standen. 1975. Potassium activation in *Helix aspersa* neurones under voltage clamp: a component mediated by calcium influx. *J. Physiol. (Lond.).* 249:211–239.

Moolenaar, W. H., and I. Spector. 1978. Ionic currents in cultured mouse neuroblastoma cells under voltage clamp conditions. *J. Physiol. (Lond.).* 278:265–286.

Moolenaar, W. H., and I. Spector. 1979. The calcium current and the activation of a slow potassium conductance in voltage-clamped mouse neuroblastoma cells. *J. Physiol. (Lond.).* 292:307–323.

Oxford, G. S., and D. J. Adams. 1981. Permeant cations after K channel kinetics and permeability. *Biophys. J.* 33:70*a*. (Abstr.)

Ozawa, S. 1981. Biphasic effect of thyrotropin-releasing hormone on membrane K^+ permeability in rat clonal pituitary cells. *Brain Res.* 209:240–244.

Ozawa, S., and N. Kimura. 1979. Membrane potential changes caused by thyrotropin-releasing hormone in the clonal GH3 cell and their relationship to secretion of pituitary hormone. *Proc. Natl. Acad. Sci. USA.* 76:6017–6020.

Ozawa, S., and S. Miyazaki. 1979. Electrical activity in the rat clonal pituitary cell and its relation to hormone secretion. *Jpn. J. Physiol.* 29:411–426.

Reuter, H., and C. F. Stevens. 1980. Ion conductance and ion selectivity of potassium channels in snail neurones. *J. Membr. Biol.* 57:103–118.

Sand, O., E. Haug, and K. M. Gautvik. 1980. Effects of thyroliberin and 4-aminopyridine on action potentials and prolactin release and synthesis in rat pituitary cells in culture. *Acta Physiol. Scand.* 108:247–252.

Sillen, L. G., and A. E. Martell. 1964. Stability Constants of Metal-Ion Complexes; Suppl. 1. Chemical Society, Burlington House, London. 733.

Taraskevich, P. S., and W. W. Douglas. 1980. Electrical behavior in a line of anterior pituitary cells (GH cells) and the influence of the hypothalamic peptide, thyrotropin-releasing factor. *Neuroscience.* 5:421–431.

Thompson, S. H. 1977. Three pharmacologically distinct potassium channels in molluscan neurones. *J. Physiol. (Lond.).* 265:465–488.

Thompson, S. H., and R. W. Aldrich. 1980. Membrane potassium channels. *In* The Cell Surface and Neuronal Function. C. W. Cotman, G. Poste, and G. L. Nicolson, editors. Elsevier/North-Holland Biomedical Press, Amsterdam. 49–85.

Tixier-Vidal, A., D. Gourdji, and C. Tougard. 1975. A cell culture approach to the study of anterior pituitary cells. *Int. Rev. Cytol.* 41:173–239.

Wong, B. S., H. Lecar, and M. Adler. 1982. Single calcium-dependent potassium channels in clonal anterior pituitary cells. *Biophys. J.* 39:313–317.

Yellen, G. 1982. Single Ca^{2+}-activated nonselective cation channels in neuroblastoma. *Nature (Lond.).* 296:357–359.